Urban Forestry & Urban Greening 114 (2025) 129171

Contents lists available at ScienceDirect

Urban Forestry & Urban Greening

journal homepage: www.elsevier.com/locate/ufug

Original article

Mobile LiDAR applications to monitor the urban forest in the city of Hasselt, Belgium

Sam Ottoy[a,b,c,*], Joanna Nedelkou[a], Ward De Witte[a,c], Alain De Vocht[a,c]

[a] PXL BIO-Research, PXL University of Applied Sciences and Arts, Diepenbeek, Belgium
[b] Division of Forest, Nature and Landscape, KU Leuven, Leuven, Belgium
[c] Center for Environmental Sciences, Hasselt University, Diepenbeek, Belgium

ARTICLE INFO

Dataset link: Mobile LiDAR time series datasets of urban trees

Keywords:
Urban forest
Remote Sensing
Mobile LiDAR
Tree Inventory
Urban Trees
Monitoring

ABSTRACT

Urban forests provide essential ecosystem services and are key components of urban policy-making. Both accounting for these ecosystem services and effective urban forest management planning, however, requires an up-to-date and detailed 3D tree inventory. Conducting and maintaining up-to-date tree inventories often involves field visits and manual recordings. In this study, we demonstrate the applicability of close-range remote sensing in measuring and monitoring tree characteristics over time. A mobile LiDAR system was deployed to collect dense point clouds (1789.92 points/m^2) in the city of Hasselt, Belgium. The proposed individual tree detection algorithm obtained a recall score of 0.84, a precision of 0.82 and an F-score of 0.83. The average estimated characteristics were: tree height (H) of 9.84 $\pm$ 2.68 m, diameter at breast height (DBH) of 0.48 $\pm$ 0.74 m, crown projection (PA) of 14.87 $\pm$ 11.60 m^2 and crown volume (AV) of 73.59 $\pm$ 98.42 m^3 . For a subset of 47 manually measured trees (r)RMSE values were 0.58 m (259 %) and 0.96 m (10 %) for DBH and H, respectively. Excluding incorrectly segmented trees mainly improved (r)RMSE values of DBH (0.05 m, 21 %) and only had a minor effect on H (0.95 m, 11 %). Two case studies based on multi-temporal MLS-datasets allowed to estimate the volume of pruning biomass and to detect a nest of Asian hornet (*Vespa velutina*). The obtained results can support both policy-making and operational planning by integrating 3D tree inventories and assessing the effect of management activities.

1. Introduction

Urban forests and individual trees provide ecosystem services that contribute to human health and the overall livability of urban environments (Wolf et al., 2020). Despite their wide range of essential benefits, these services are often not taken into account in urban policy planning. Recently, the 3–30–300 rule (Konijnendijk, 2023) and the EU Nature Restoration Law are more and more inspiring policy makers, but implementing these concepts require the availability of an up-to-date and detailed tree inventory with information about the location and 2D-/3D-characteristics (such as tree height, crown projection and crown volume) of the trees (Browning et al., 2024). In addition, such detailed urban tree inventories form the basis for effective policy and management planning (Ma et al., 2021; Östberg et al., 2018) and can be used to assess ecosystem services (Rahman et al., 2020; Sharma et al., 2025) and disservices (Masini et al., 2023). Nielsen et al. (2014) distinguished four main types of urban tree inventories of which three are based on remote sensing (satellite-supported, airplane-supported and on-the-ground scanning or digital photography). The fourth category, field surveys, was still the most popular, despite being labor-intensive and time-consuming (Nielsen et al., 2014) and susceptible to observer bias (Degerickx et al., 2018). In contrast, inventory campaigns using remote sensing data can be less costly than and more standardized than these traditional field visits (Ma et al., 2021; Saarinen et al., 2014). Recent studies highlighted the potential of satellite (Marcilio-Silva et al., 2025; Zhao et al., 2024) and airborne (Wallace et al., 2021; Yun et al., 2021) remote sensing for updating urban tree inventories. These approaches, however, are often not detailed enough to capture the full 3D structure of a tree, and hence allow to monitor management activities such as tree pruning.

Recent research shows that close-range remote sensing data are capable of measuring various characteristics at the tree level and monitoring them efficiently over time (Chen et al., 2024; Qi et al., 2022). Further development of LiDAR (Light Detection and Ranging) remote

* Correspondence to: PXL BIO-Research, PXL University of Applied Sciences and Arts, Agoralaan H, 3590 Diepenbeek, Belgium.
E-mail address: Sam.Ottoy@pxl.be (S. Ottoy).

https://doi.org/10.1016/j.ufug.2025.129171
Received 14 June 2025; Received in revised form 17 October 2025; Accepted 9 November 2025
Available online 10 November 2025

sensing via Unmanned Aerial Vehicles (UAVs) or mobile platforms stimulated the generation of highly accurate 3D models of trees (Hu et al., 2022). In this context, dense point clouds (+500 points/m^2) can be generated from which 3D structures can be derived (Hu et al., 2022; Qi et al., 2022). In particular, for Mobile LiDAR Systems (MLS) to be useful in operational urban tree mapping, Holopainen et al. (2013) expressed the need for improvements in processing methodologies and data collection.

The main objectives of this study were to evaluate the capacity of close-range remote sensing based on MLS to (i) detect individual trees in a highly urbanized region, (ii) assess the successive derivation of various tree characteristics which are required for efficient tree management, and (iii) monitor these characteristics over time in two individual case studies. Objectives (i) and (ii) will serve policy-making and design of urban forestry at the city level (a.o. based on quantitative assessments of the 3–30–300 rule), whereas objective (iii) deals with the operational level of monitoring and evaluating tree management activities.

2. Material and methods

2.1. Study site and data collection

The study focused on all trees next to the R70 street in Hasselt, Belgium. This street has the shape of an (inner) ring with a length of 2.5 km. It contains 451 trees, with a dominance of *Acer platanoides* (319 trees or 70.73 %). MLS data collection was carried out in March and December 2024 with a YellowScan Surveyor Ultra (HESAI XT32M2X) attached to a car, which was driving approximately 50 km/h. The LiDAR sensor has a pulse rate of 640k shots per second (20 k x 32 beams) and a field of view of 360°.

2.2. Individual tree detection

After data collection, the raw point clouds were processed in sensor-specific YellowScan's CloudStation software version 2409.0.0. The trajectory was postprocessed with Applanix' POSPac MMS (version 8.9), which included the determination of the Smooth Best Estimated Trajectory (SBET) based upon the sensor's lever arms and the local RTK network FLEPOS (Flemish Positioning Service). After SBET processing, strip adjustment was performed based on the integrated 'Drive' method, and classification of the point cloud (ground vs. non-ground) was carried out with a minimal object height of 0.15 m and a default point cloud thickness of 0.10 m. The resulting point clouds (in .las format and projected in the CRS UTM 31 N, EPSG:32631) were exported, since further processing was done in R-software (version 4.3.2).

In line with the procedure applied in a previous study focusing on individual tree detection (ITD) in tree nurseries (Ottoy et al., 2022), the resulting point clouds were first normalized based on the *normalize_height* function of the lidR-package (Roussel et al., 2020). Points representing noise were classified with the *classify_noise* function in combination with Statistical Outlier Removal (SOR), and removed from the point cloud. Next, treetops were determined at point cloud level using the *locate_trees* function in combination with a local maximum filter (*lmf*) with a minimum tree height of 5 m and a variable window size depending on the tree height (Formula 1). The variable window size will allow larger search areas for taller trees to detect their treetops.

$$Crown\ radius(m) = 3 + 0.1 * Tree\ height(m) \tag{1}$$

The identified treetops were used to segment trees using the algorithm of Silva et al. (2016). This resulted in a point cloud for each detected tree. Since the overall point cloud still contained other street infrastructure besides trees, such as lampposts, traffic signs and parked cars an additional filter was applied. The compactness (S) of each tree crown was computed based on the polygon shape index using Formula 2. A circle is seen as the most compact shape and has an S-value of 1. Assuming trees in an urban environment have a rather round shape, only objects with an S-value < 1.15 were included for further analyses. In addition, objects consisting of less than 1000 points were omitted. These objects were stored separately to allow verification in a later phase.

$$S = \sqrt{\frac{Perimeter^2}{4 * \pi * Area}} \tag{2}$$

Individual tree characteristics were computed using the *summary_basic_pointcloud_metrics* function of the ITSMe-package (Terryn et al., 2023). This function computed tree height (H in m), diameter at breast height (DBH in m), crown projection (PA in m^2) and crown volume (AV in m^3). A graphical overview of the applied methodology is presented in Fig. 1.

2.3. Validation

The accuracy of the individual tree detection workflow was tested by computing the number of trees that were detected correctly (true positive, TP), omitted (false negative, FN) and committed (false positive, FP). The available tree inventory of the city of Hasselt served as the reference dataset for this analysis. Next, recall (Formula 3), precision (Formula 4) and F-score (Formula 5) metrics were computed. Whereas recall can be used as a measure of the tree detection rate, precision indicates the correctness of the detected trees. The F-score is an overall summary of individual tree detection performance and, ranges between 0 (none of the trees detected) and 1 (all trees detected without FPs).

$$r = \frac{TP}{TP + FN} \tag{3}$$

$$p = \frac{TP}{TP + FP} \tag{4}$$

$$F = \frac{2 * r * p}{r + p} \tag{5}$$

In April 2024, 47 trees were manually measured (Fig. 2). Diameter at breast height (DBH) was measured with a tape measure, whereas tree height was measured with a laser rangefinder (Nikon Forestry Pro II, Nikon, Tokyo, Japan) with an accuracy of 0.3 m. The latter is frequently used in field conditions by urban foresters and arborists (Martin, 2022) and can as such serve as a useful validation tool. These observations were used to compute Root Mean Squared Errors (RMSE) and relative RMSE (rRMSE) values.

2.4. Time series analysis

Applying the workflow described in Section 2.2 on the MLS datasets from the two collection dates (March 2024 and December 2024), allowed us to monitor the effect of management activities. In this context, particular attention is given to assessing the amount of removed biomass due to pruning activities. Given the precise georeferencing of the generated point clouds, point clouds of individual trees could be geomatched using the two datasets.

3. Results

3.1. Individual tree detection

The generated point cloud of the street network covering an area of 79452 m^2 consisted of 142.21 million points, resulting in an average point density of 1789.92 points per m^2. The proposed method identified a total of 464 trees, of which 379 were true positives and 85 false positives. A total of 72 trees were not detected correctly (FN). This resulted in a recall score of 0.84, a precision of 0.82 and an overall F-score of 0.83. For each tree, tree characteristics were derived (Fig. 3). The average estimated tree characteristics were; tree height (H) of 9.84 $\pm$ 2.68 m, diameter at breast height (DBH) of 0.48 $\pm$ 0.74 m, crown

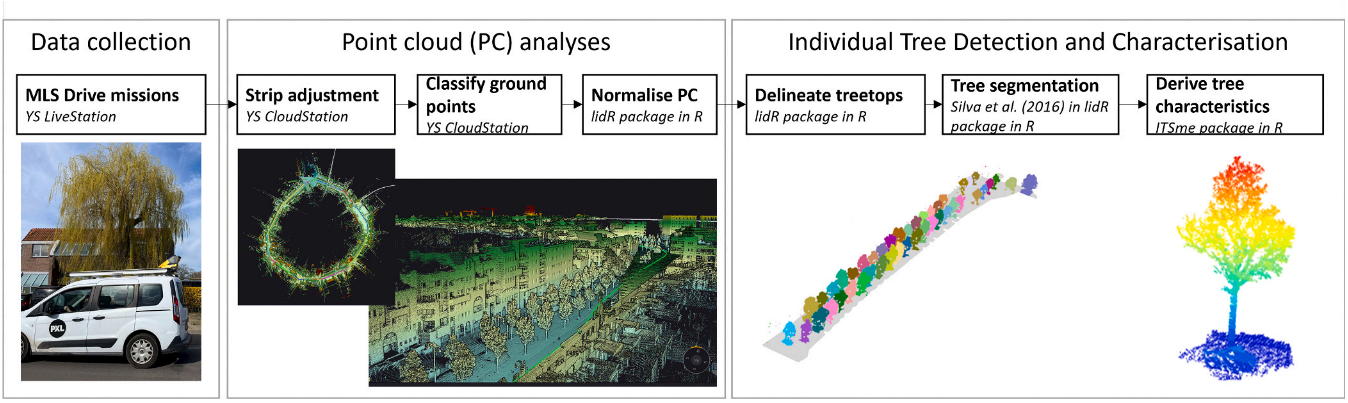

Fig. 1. Graphical overview of the applied procedure consisting of three steps: data collection, point cloud analyses and individual tree detection and characterisation.

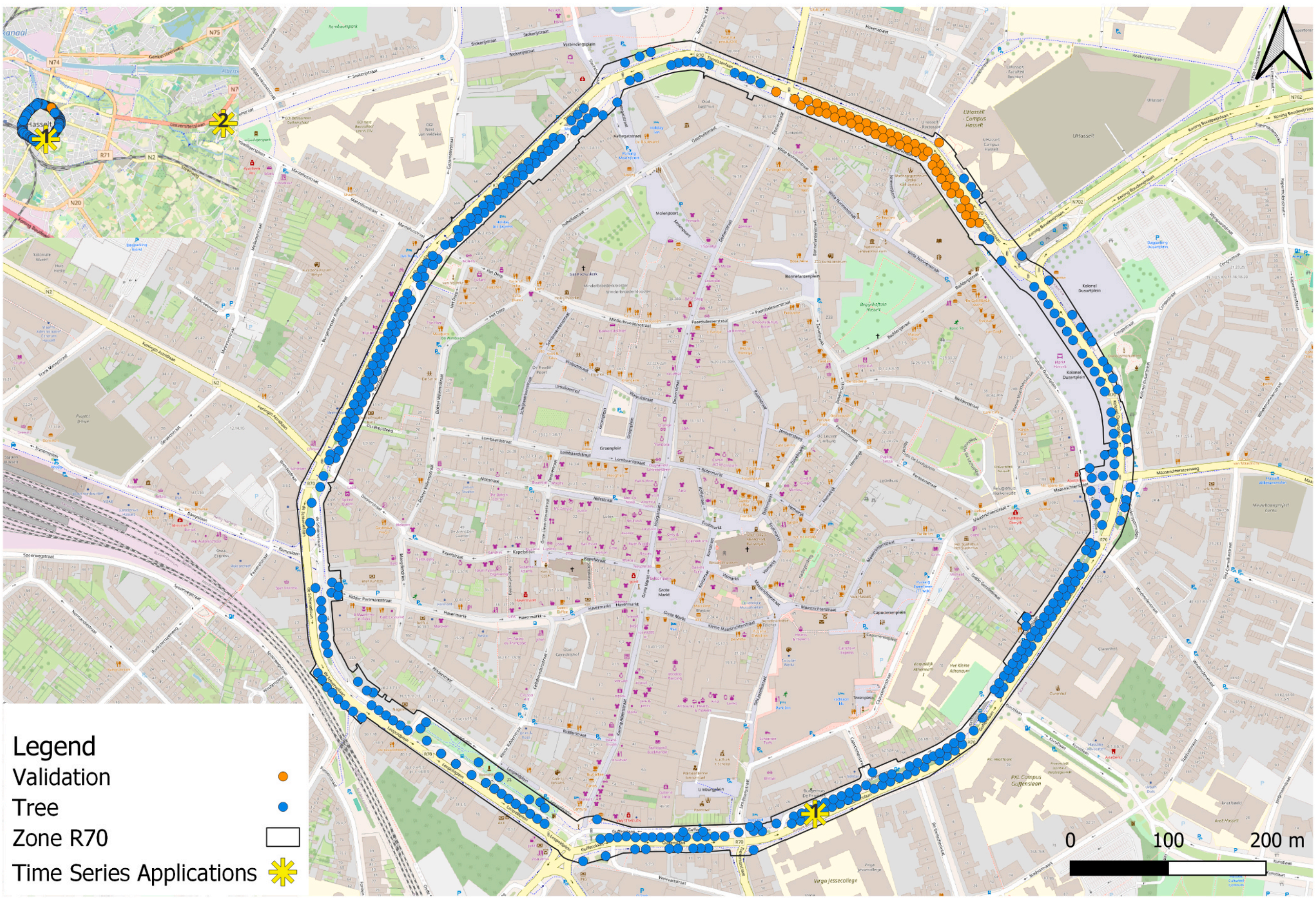

Fig. 2. Overview of the R70 street in the city of Hasselt and the trees present in the reference dataset. Trees which were visited for validation of tree height and diameter estimates are presented in orange. Time series applications comprise the detection of an Asian hornet nest (1) and a pruning assessment (2).

projection of 14.87 ± 11.60 m^2 and crown volume of 73.59 ± 98.42 m^3 (Table 1). For the subset of 47 trees for which measured H and DBH values were available, the height of all trees could be estimated, whereas the stem diameter of 5 trees could not be estimated, and the diameter estimate of 7 additional trees was clearly disturbed as a consequence of an incorrect segmentation due to the presence of street infrastructure (Fig. 4 A and 4B). This resulted in (r)RMSE values of 0.58 m (259 %) and 0.96 m (10 %) for DBH and H, respectively. Excluding the 7 incorrectly segmented trees altered (r)RMSE values to 0.05 m (21 %) and 0.95 m (11 %) for DBH and H, respectively.

3.2. Time series applications

Focusing on two particular situations in which multi-temporal point clouds are available, we were able to estimate the amount of pruning volume (Fig. 5). Before pruning (March 2024), the tree of interest was characterized by a crown projection of 75 m^2 and a crown volume of 479 m^3 . After pruning (December 2024), the crown projection showed a minor decrease (11 %, to 67 m^2), whereas the crown volume decreased by 38 % to 297 m^3 . Similarly, by comparing time series of point clouds, we were able to detect a nest of Asian Hornet (*Vespa velutina*), Fig. 6. This nest was not only characterized by a circular shape, but also by

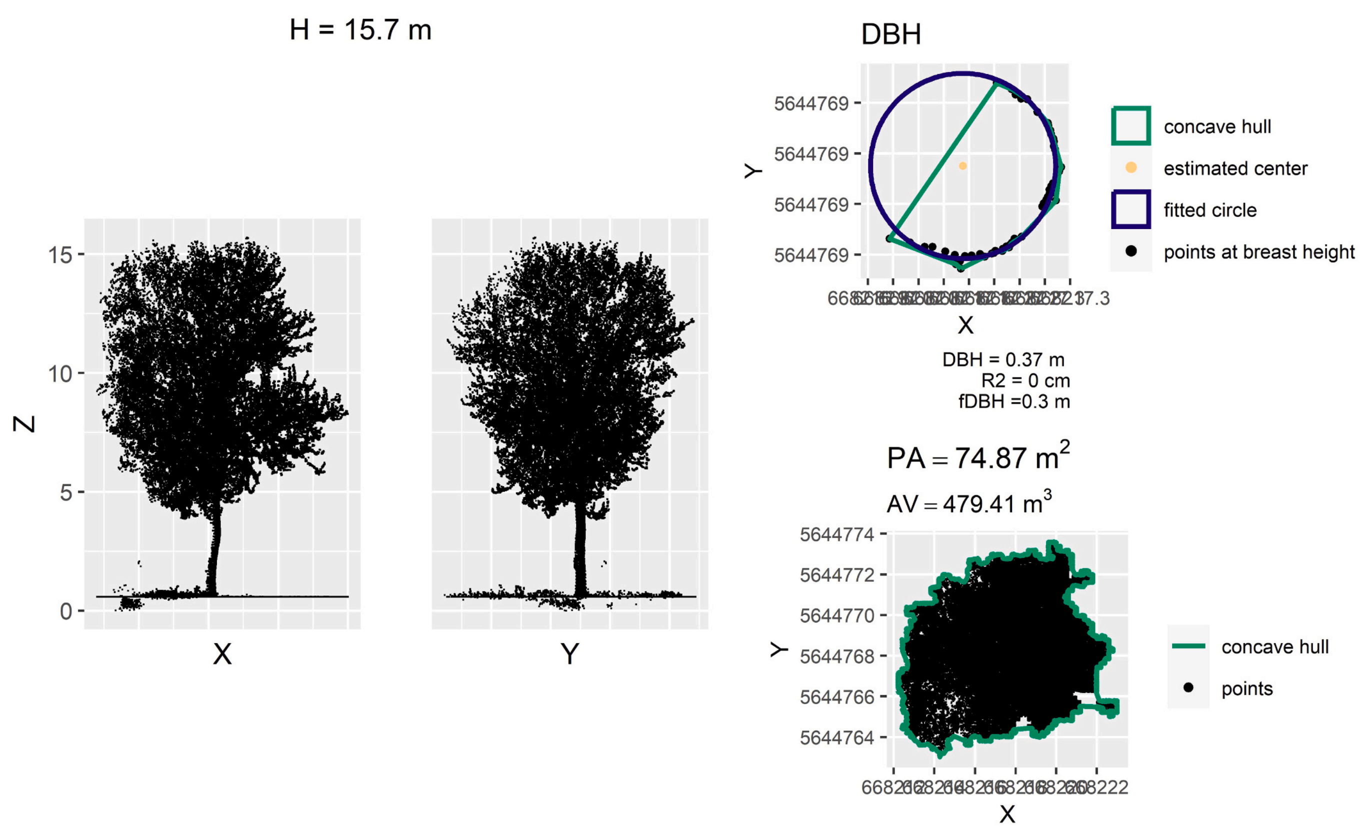

Fig. 3. Graphical result of the estimated tree characteristics using the *summary_basic_pointcloud_metrics* function of the ITSMe-package (Terryn et al., 2023), with tree height (H), diameter at breast height (DBH), crown projection (PA) and crown volume (AV).

Table 1
Overview of estimated tree characteristics. The full dataset contained 379 correctly detected trees. The reference subset contained 47 trees with measured H and DBH values.

Tree characteristic	Full dataset		Reference subset			
	Average estimated	Standard Deviation	Average estimated	Average measured	RMSE	rRMSE
Tree height (H, m)	9.84	2.68	9.39	9.19	0.96	259.61 %
Diameter at breast height (DBH, m)	0.48	0.74	0.46	0.22	0.58	10.40 %
Crown projection (PA, m^2)	14.87	11.60	10.75	/	/	/
Crown volume (AV, m^3)	73.59	98.42	42.31	/	/	/

increased LiDAR-intensity values. Both time series are available in Mendeley Data (doi: 10.17632/cw2ynn4bfv.1).

4. Discussion

The ITD performance metrics are in line with those observed in studies focusing on medium-density forest stands (Young et al., 2022). Whereas the F-score of ITD in high-density forests can be lower (0.44), F-scores of 0.94 were found in low-density stands (Belmonte et al., 2020). Similarly, the F-score of taxus tree nurseries, which are typically characterized by low densities, non-overlapping crowns and a lack of other infrastructure, was found to be higher in a previous study (0.88 – 0.99 in Ottoy et al. (2022)). Focusing on urban forests, Holopainen et al. (2013) found that MLS was capable of detecting 26.94–79.22 % of the trees correctly, with an automatic and manual approach, respectively. Even though trees in an urban context are typically regularly spaced, and tree crowns are rarely overlapping, the presence of additional infrastructure poses additional challenges in the segmentation performance of the resulting point clouds (Jiang et al., 2022). In this context, it should also be noted that the algorithm of Silva et al. (2016) used in this study originates from a (longleaf pine) forestry context and as such does not readily address these urban challenges. This resulted in higher rRMSE values for DBH estimates compared to H estimates. Further improvements can thus be situated in the field of tree segmentation, e.g. taking benefit from deep learning and data fusion approaches (Chi et al., 2025; Ferreira et al., 2024; Pu and Landry, 2020) and are necessary to increase the potential for widespread use of MLS.

From the subset of 47 reference trees, the DBH of 5 trees could not be estimated, while the DBH estimation of 7 additional trees was disturbed due to the presence of street infrastructure in the radius of the tree crown. Omitting these trees improved (r)RMSE to 0.05 m (21 %) compared to 0.57 m (259 %), which is in line with values observed by Heo et al., (2019), who obtained DBH-RMSE values of 0.0377 m for street trees and 0.0895 cm for park trees. It should be noted that due to the one-way direction and design of the street network, trees could only be passed by one side, which resulted in semicircles representing the tree trunk. Even though the algorithm was capable of fitting a circle to estimate DBH, this process can be error-prone. Also, for the comparison of tree height, caution is required given potential quality issues with the reference data as the result of the accuracy of the laser rangefinder (0.30 m according to the producer’s manual) and the effects of incorrectly placed pivot points (Andersen et al., 2006) and the position of the

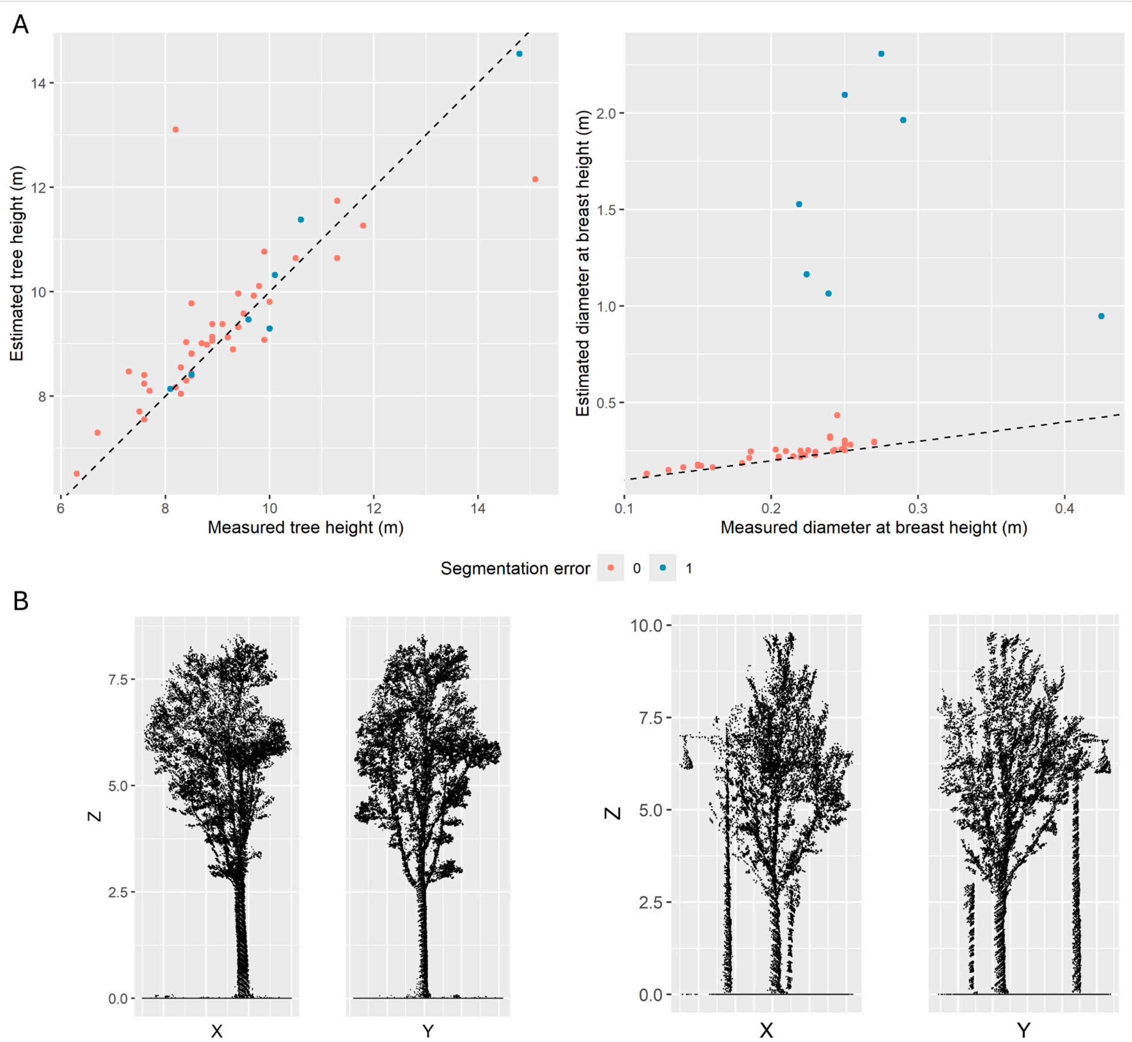

Fig. 4. (A) Overview of measured and estimated tree characteristics: tree height and diameter at breast height. (B) Illustration of a correctly segmented tree point cloud (left) and an infrastructure affected tree point cloud (right).

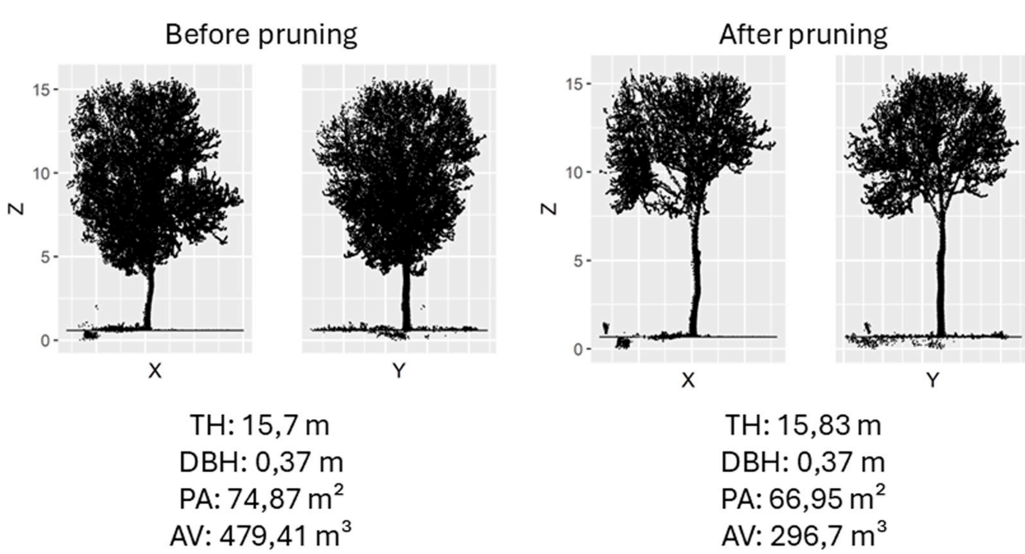

Fig. 5. Point clouds of a tree before (left) and after (right) pruning, with estimation of tree height (H), diameter at breast height (DBH), crown projection (PA) and crown volume (AV).

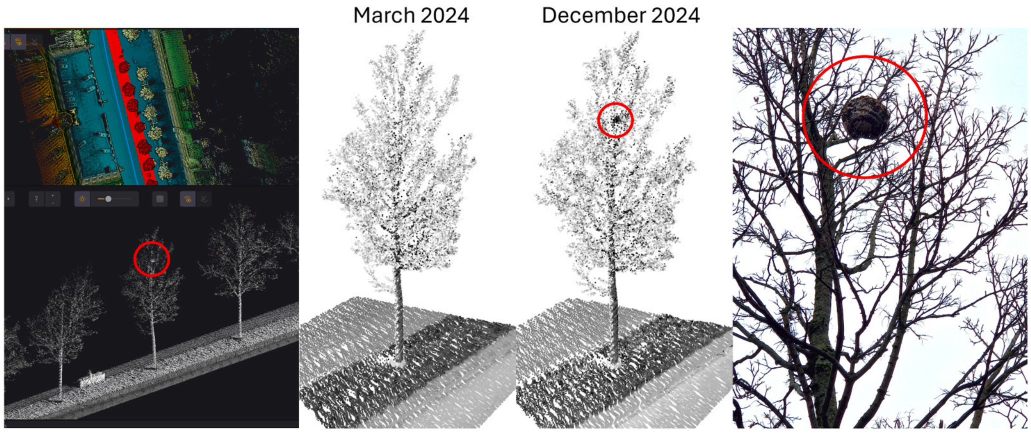

Fig. 6. Graphical representation of the tree without (March 2024) and with (December 2024) Asian hornet nest. The point clouds are coloured by intensity values.

treetop with respect to the base of the tree (Saliu et al., 2021). Under- or overestimation of tree heights impedes a proper comparison of the results. In addition, as mentioned before, more advanced segmentation techniques can overcome estimation errors induced by the presence of other urban infrastructures in the tree point clouds. Urban forest inventories derived from close-range remote sensing can be useful inputs in the training process of solutions based on satellite (Baines et al., 2020) or airborne (Pires et al., 2024) remote sensing.

The availability of time series of point clouds can support urban tree management and planning, especially by giving insights into the impacts of management activities and decisions. According to the European Tree Pruning Standard (EAS, 2024), leaf area removal in formative pruning operations in young to semi-mature trees with a temporary crown should not exceed 30 %. More intense pruning could damage the tree and impact its physiological condition. Quantitative information about adopting and adhering to this rule is, however, often lacking. Our insights can provide the city administration with the necessary datasets and corresponding toolbox to (i) check whether management activities have been carried out according to the local regulations, and (ii) increase the effectiveness of law enforcement in case the regulation has not been adopted accordingly. Additionally, time series can support (early, depending on the time frequency of data collection) detection systems for the presence of Asian hornet nests. In this context, Turchi and Derijard, (2018) pointed to the need to optimize nest detection techniques. Even though this was not the main goal of this study, our explorative results show the potential of close-range LiDAR remote sensing, e.g. to include in data fusion approaches with thermal (Lioy et al., 2021) and hyperspectral (Song et al., 2025) imagery.

5. Conclusions

Our study shows the added value of MLS for urban tree detection, characterization, and monitoring. While the method has the potential for identifying individual trees and estimating 3D characteristics, challenges related to segmentation accuracy and the presence of urban infrastructure highlight the need for further advancements in data processing techniques. The ability to generate high-density point clouds over time presents new opportunities for urban forest planning and management, allowing policymakers to assess compliance with regulations such as the 3–30–300 rule and tree pruning standards. By integrating such technologies into urban planning, cities can enhance the efficiency of tree inventories and improve decision-making processes by explicitly considering the three dimensionalities of the urban forest.

CRediT authorship contribution statement

Alain De Vocht: Writing – review & editing, Project administration, Funding acquisition. **Ward De Witte:** Writing – review & editing, Validation, Methodology, Conceptualization. **Joanna Nedelkou:** Writing – review & editing, Visualization, Methodology. **Sam Ottoy:** Writing – review & editing, Writing – original draft, Visualization, Validation, Methodology, Investigation, Formal analysis, Conceptualization.

Declaration of Competing Interest

The authors declare that they have no known competing financial interests or personal relationships that could have appeared to influence the work reported in this paper.

Acknowledgements

We acknowledge the support of the city administration of Hasselt.

Data availability

Mobile LiDAR time series datasets of urban trees (Mendeley Data)

References

Andersen, H.-E., Stephen E, R., McGaughey, R.J., 2006. A rigorous assessment of tree height measurements obtained using airborne lidar and conventional field methods. Can. J. Remote Sens. 32, 355–366. https://doi.org/10.5589/m06-030.

Baines, O., Wilkes, P., Disney, M., 2020. Quantifying urban forest structure with open-access remote sensing data sets. Urban Urban Green. 50, 126653. https://doi.org/10.1016/j.ufug.2020.126653.

Belmonte, A., Sankey, T., Biederman, J.A., Bradford, J., Goetz, S.J., Kolb, T., Woolley, T., 2020. UAV-derived estimates of forest structure to inform ponderosa pine forest restoration. Remote Sens Ecol. Conserv 6, 181–197. https://doi.org/10.1002/rse2.137.

Browning, M.H.E.M., Locke, D.H., Konijnendijk, C., Labib, S.M., Rigolon, A., Yeager, R., Bardhan, M., Berland, A., Dadvand, P., Helbich, M., Li, F., Li, H., James, P., Klompmaker, J., Reuben, A., Roman, L.A., Tsai, W.-L., Patwary, M., O'Neil-Dunne, J., Ossola, A., Wang, R., Yang, B., Yi, L., Zhang, J., Nieuwenhuijsen, M., 2024. Measuring the 3-30-300 rule to help cities meet nature access thresholds. Sci. Total Environ. 907, 167739. https://doi.org/10.1016/j.scitotenv.2023.167739.

Chen, J., Liang, X., Liu, Z., Gong, W., Chen, Y., Hyyppä, J., Kukko, A., Wang, Y., 2024. Tree species recognition from close-range sensing: a review. Remote Sens. Environ. 313, 114337. https://doi.org/10.1016/j.rse.2024.114337.

Chi, D., Yan, J., Yu, K., Morsdorf, F., Somers, B., 2025. Planting contexts affect urban tree species classification using airborne hyperspectral and LiDAR imagery. Land. Urban Plan 257, 105316. https://doi.org/10.1016/j.landurbplan.2025.105316.

Degerickx, J., Roberts, D.A., McFadden, J.P., Hermy, M., Somers, B., 2018. Urban tree health assessment using airborne hyperspectral and LiDAR imagery. Int. J. Appl. Earth Obs. Geoinf. 73, 26–38. https://doi.org/10.1016/j.jag.2018.05.021.

EAS, 2024. EAS 01:2024 (EN) – European Tree Pruning Standard.

Ferreira, M.P., dos Santos, D.R., Ferrari, F., Coelho, L.C.T., Martins, G.B., Feitosa, R.Q., 2024. Improving urban tree species classification by deep-learning based fusion of digital aerial images and LiDAR. Urban Urban Green. 94, 128240. https://doi.org/10.1016/j.ufug.2024.128240.

Heo, H.K., Lee, D.K., Park, J.H., Thorne, J.H., 2019. Estimating the heights and diameters at breast height of trees in an urban park and along a street using mobile LiDAR. Landsc. Ecol. Eng. 15, 253–263. https://doi.org/10.1007/s11355-019-00379-6.
Holopainen, M., Kankare, V., Vastaranta, M., Liang, X., Lin, Y., Vaaja, M., Yu, X., Hyyppä, J., Hyyppä, H., Kaartinen, H., Kukko, A., Tanhuanpää, T., Alho, P., 2013. Tree mapping using airborne, terrestrial and mobile laser scanning – A case study in a heterogeneous urban forest. Urban Urban Green. 12, 546–553. https://doi.org/10.1016/j.ufug.2013.06.002.
Hu, T., Wei, D., Su, Y., Wang, X., Zhang, J., Sun, X., Liu, Y., Guo, Q., 2022. Quantifying the shape of urban street trees and evaluating its influence on their aesthetic functions based on mobile lidar data. ISPRS J. Photogramm. Remote Sens. 184, 203–214. https://doi.org/10.1016/j.isprsjprs.2022.01.002.
Jiang, T., Wang, Y., Liu, S., Cong, Y., Dai, L., Sun, J., 2022. Local and Global Structure for Urban ALS point cloud semantic segmentation with ground-aware attention. IEEE Trans. Geosci. Remote Sens. 60, 1–15. https://doi.org/10.1109/TGRS.2022.3158362.
Konijnendijk, C.C., 2023. Evidence-based guidelines for greener, healthier, more resilient neighbourhoods: Introducing the 3–30–300 rule. J. Res (Harbin) 34, 821–830. https://doi.org/10.1007/s11676-022-01523-z.
Lioy, S., Bianchi, E., Biglia, A., Bessone, M., Laurino, D., Porporato, M., 2021. Viability of thermal imaging in detecting nests of the invasive hornet Vespa velutina. Insect Sci. 28, 271–277. https://doi.org/10.1111/1744-7917.12760.
Ma, B., Hauer, R.J., Östberg, J., Koeser, A.K., Wei, H., Xu, C., 2021. A global basis of urban tree inventories: What comes first the inventory or the program. Urban Urban Green. 60, 127087. https://doi.org/10.1016/j.ufug.2021.127087.
Marcilio-Silva, V., Donovan, S., Hobbie, S.E., Guzmán, Q., Knight, J.A., Cavender-Bares, J, J.F., 2025. Integrating remote sensing and field inventories to understand determinants of urban forest diversity and structure. Ecology 106, e70020. https://doi.org/10.1002/ecy.70020.
Martin, A.J.F., 2022. Accuracy and precision in urban forestry tools for estimating total tree height. Arboric. Urban For. (AUF) 48, 319–332. https://doi.org/10.48044/jauf.2022.024.
Masini, E., Tomao, A., Corona, P., Fattorini, L., Giuliarelli, D., Portoghesi, L., Agrimi, M., 2023. The ecosystem disservices of trees on sidewalks: a study based on a municipality urban tree inventory in Central Italy. Urban Urban Green. 86, 128007. https://doi.org/10.1016/j.ufug.2023.128007.
Nielsen, A., Östberg, J., Delshammar, T., 2014. Review of urban tree inventory methods used to collect data at single-tree level. Arboric. Urban 40. https://doi.org/10.48044/jauf.2014.011.
Östberg, J., Wiström, B., Randrup, T.B., 2018. The state and use of municipal tree inventories in Swedish municipalities – results from a national survey. Urban Ecosyst. 21, 467–477. https://doi.org/10.1007/s11252-018-0732-3.
Ottoy, S., Tziolas, N., Van Meerbeek, K., Aravidis, I., Tilkin, S., Sismanis, M., Stavrakoudis, D., Gitas, I.Z., Zalidis, G., De Vocht, A., 2022. Effects of flight and smoothing parameters on the detection of taxus and olive trees with UAV-borne imagery. Drones 6. https://doi.org/10.3390/drones6080197.
Pires, R., de, Lindberg, P., Persson, E., Olofsson, H.J., Holmgren, J, K., 2024. Mobile laser scanning as reference for estimation of stem attributes from airborne laser scanning. Remote Sens Environ. 315, 114414. https://doi.org/10.1016/j.rse.2024.114414.
Pu, R., Landry, S., 2020. Mapping urban tree species by integrating multi-seasonal high resolution pléiades satellite imagery with airborne LiDAR data. Urban Urban Green. 53, 126675. https://doi.org/10.1016/j.ufug.2020.126675.
Qi, Y., Coops, N.C., Daniels, L.D., Butson, C.R., 2022. Comparing tree attributes derived from quantitative structure models based on drone and mobile laser scanning point clouds across varying canopy cover conditions. ISPRS J. Photogramm. Remote Sens. 192, 49–65. https://doi.org/10.1016/j.isprsjprs.2022.07.021.
Rahman, M.A., Stratopoulos, L.M.F., Moser-Reischl, A., Zölch, T., Häberle, K.-H., Rötzer, T., Pretzsch, H., Pauleit, S., 2020. Traits of trees for cooling urban heat islands: a meta-analysis. Build. Environ. 170, 106606. https://doi.org/10.1016/j.buildenv.2019.106606.
Roussel, J.-R., Auty, D., Coops, N.C., Tompalski, P., Goodbody, T.R.H., Meador, A.S., Bourdon, J.-F., de Boissieu, F., Achim, A., 2020. lidR: an R package for analysis of Airborne Laser Scanning (ALS) data. Remote Sens. Environ. 251, 112061. https://doi.org/10.1016/j.rse.2020.112061.
Saarinen, N., Vastaranta, M., Kankare, V., Tanhuanpää, T., Holopainen, M., Hyyppä, J., Hyyppä, H., 2014. Urban-tree-attribute update using multisource single-tree inventory. Forests 5, 1032–1052. https://doi.org/10.3390/f5051032.
Saliu, I.S., Satyanarayana, B., Bin Fisol, M.A., Wolswijk, G., Decannière, C., Lucas, R., Otero, V., Dahdouh-Guebas, F., 2021. An accuracy analysis of mangrove tree height mensuration using forestry techniques, hypsometers and UAVs. Estuar. Coast Shelf Sci. 248, 106971. https://doi.org/10.1016/j.ecss.2020.106971.
Sharma, G., Morgenroth, J., Richards, D.R., Ye, N., 2025. Advancing urban forest and ecosystem service assessment through the integration of remote sensing and i-Tree Eco: a systematic review. Urban Urban Green. 104, 128659. https://doi.org/10.1016/j.ufug.2024.128659.
Silva, C.A., Hudak, A.T., Vierling, L.A., Loudermilk, E.L., O'Brien, J.J., Hiers, J.K., Jack, S.B., Gonzalez-Benecke, C., Lee, H., Falkowski, M.J., Khosravipour, A., 2016. Imputation of individual longleaf pine (Pinus palustris Mill.) tree attributes from field and LiDAR data. Can. J. Remote Sens. 42, 554–573. https://doi.org/10.1080/07038992.2016.1196582.
Song, W., Kim, H., Kim, W., 2025. Modeling urban wasp nest occurrences using 119 fire service reports, LiDAR, and hyperspectral imagery: the role of green spaces and structural factors. J. Environ. Manag. 379, 124776. https://doi.org/10.1016/j.jenvman.2025.124776.
Terryn, L., Calders, K., Åkerblom, M., Bartholomeus, H., Disney, M., Levick, S., Origo, N., Raumonen, P., Verbeeck, H., 2023. Analysing individual 3D tree structure using the R package ITSMe. Methods Ecol. Evol. 14, 231–241. https://doi.org/10.1111/2041-210X.14026.
Turchi, L., Derijard, B., 2018. Options for the biological and physical control of Vespa velutina nigrithorax (Hym.: Vespidae) in Europe: a review. J. Appl. Entomol. 142, 553–562. https://doi.org/10.1111/jen.12515.
Wallace, L., Sun, Q. (Chayn), Hally, B., Hillman, S., Both, A., Hurley, J., Martin Saldias, D.S., 2021. Linking urban tree inventories to remote sensing data for individual tree mapping. Urban Urban Green. 61, 127106. https://doi.org/10.1016/j.ufug.2021.127106.
Wolf, K.L., Lam, S.T., McKeen, J.K., Richardson, G.R.A., van den Bosch, M., Bardekjian, A.C., 2020. Urban trees and human health: a scoping review. Int J. Environ. Res Public Health 17. https://doi.org/10.3390/ijerph17124371.
Young, D.J.N., Koontz, M.J., Weeks, J., 2022. Optimizing aerial imagery collection and processing parameters for drone-based individual tree mapping in structurally complex conifer forests. Methods Ecol. Evol. 13, 1447–1463. https://doi.org/10.1111/2041-210X.13860.
Yun, T., Jiang, K., Li, G., Eichhorn, M.P., Fan, J., Liu, F., Chen, B., An, F., Cao, L., 2021. Individual tree crown segmentation from airborne LiDAR data using a novel Gaussian filter and energy function minimization-based approach. Remote Sens Environ. 256, 112307. https://doi.org/10.1016/j.rse.2021.112307.
Zhao, X., Hu, W., Han, J., Wei, W., Xu, J., 2024. Urban above-ground biomass estimation using GEDI laser data and optical remote sensing images. Remote Sens. 16. https://doi.org/10.3390/rs16071229.